Idaho
National
Engineering
Laboratory

Managed
by the U.S.
Department
of Energy

EGG-TMI-7956
July 1987

INFORMAL REPORT **PATENT CLEARED**

THE TMI-2 CORE RELOCATION - HEAT TRANSFER AND MECHANISM

M. Epstein
H. K. Fauske

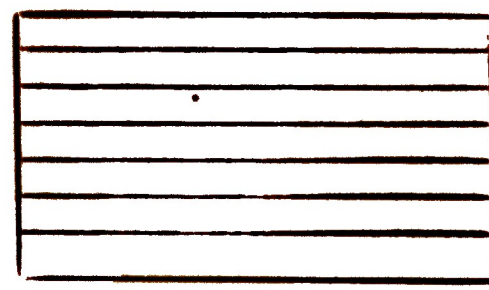

EG&G Idaho

Work performed under
DOE Contract
No. DE-AC07-76ID01570

EGG-TMI-7956

THE TMI-2 CORE RELOCATION - HEAT TRANSFER AND MECHANISM

July 1987

M. Epstein
H. K. Fauske
Fauske & Associates, Inc.
16W070 West 83rd Street
Burr Ridge, IL 60521

Prepared for:
EG&G Idaho, Inc.
Under Subcontract No. C86-131221

Work supported by the U. S. Department of Energy,
Assistant Secretary for Nuclear Energy
Office of LWR Safety and Technology
Under DOE Contract No. DE-AC07-76ID01570

ABSTRACT

It is postulated that the collapse of the upper debris bed was the main cause of core failure and core material relocation during the TMI-2 accident. It is shown that this mechanism of core relocation can account for the timescale(s) and energy transfer rate inferred from plant instrumentation. Additional analysis suggests that the water in the lower half of the reactor vessel was subcooled at the onset of relocation, as subcooling serves to explain the final coolable configuration at the bottom of the TMI vessel.

TABLE OF CONTENTS

LIST OF FIGURES

1.0 INTRODUCTION

In order to understand the core relocation event during the TMI-2 accident it is necessary to couple in-core instrument readings and vessel inspection data with an effort devoted to (i) a theoretical description and rationalization of the observations, and (ii) suggestion of any re-orientation of the vessel inspection work in those directions theoretical analyses indicate to be most likely to improve the state of TMI accident scenario knowledge. The present report describes the results of such a program, with emphasis on refinement and quantification of earlier ideas on the mechanism of core failure and the thermal-mechanical interaction of the relocating molten core material with the water in the reactor vessel.

Data from plant instrumentation recorded during the accident, the results from vessel inspections and core boring operations, and best-estimate analyses of the accident [1-3] have led to the hypothesized core configuration at 175-180 min into the accident shown schematically in Figure 1-1. The hemispherical-like region is believed to be the result of the draining and refreezing of cladding and fuel. The bottom of the hemispherical, ceramic agglomerate is about 0.7 m above the bottom of the active core, which is consistent with estimates of the liquid level in the core earlier in the accident. The initial draining of core material and the consequent diversion of steam flow to the core periphery probably resulted in the hemispherical shape of the lower surface of the ceramic agglomerate (i.e., self-crucible formation). Presumably the dense agglomerate was sufficiently hot and of such low permeability to be impervious to cooling water. A rubble bed of fragmented fuel rod material, composed of oxidized cladding and solid UO_2 rested on the upper surface of the dense ceramic agglomerate. This debris bed is believed to be the direct result of the primary coolant pump transient at 174 min. The thermal and mechanical interaction of the injected water with the hot and by this time brittle fuel probably fragmented the fuel rods and produced the debris bed. Combined video and core bore inspections revealed undamaged fuel rods around most of the periphery of the core and beneath the ceramic agglomerate. It is likely

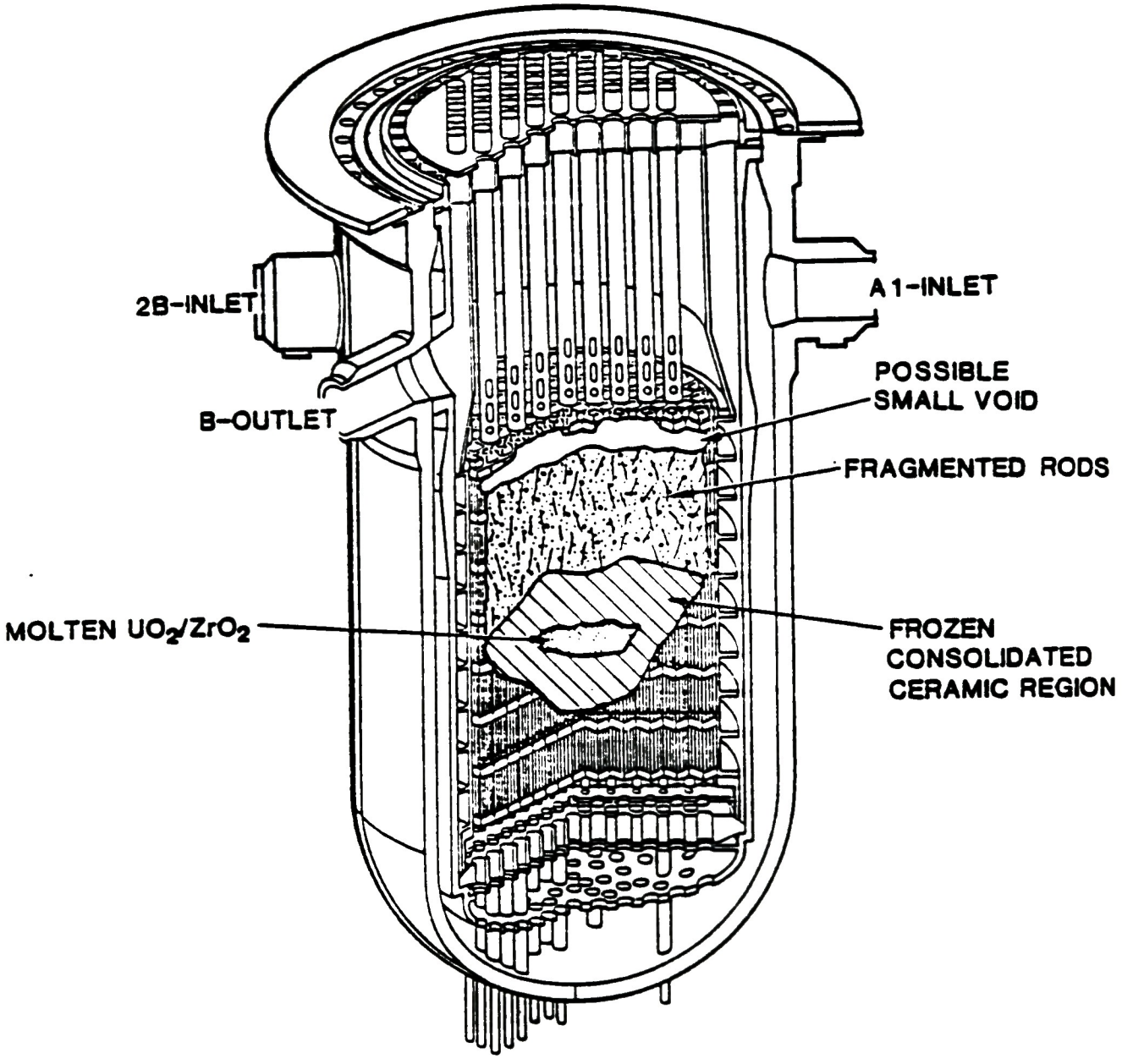

Figure 1-1 Hypothesized core damage configuration at 175-180 min. (just after B-pump transient), from Ref. [2].

that these fuel rods acted as supports and held the ceramic agglomerate in place.

At approximately 224 min into the accident the plant instrumentation conveyed strong evidence that molten core material relocated to the lower plenum. The in-core self-powered neutron detectors alarmed, the count rate on one of the neutron source-range monitors suddenly increased, and the primary system pressure jumped by about 2MPa in about 1 min. In this report an attempt is made to show that the salient qualitative and quantitative features of the available vessel examination and plant instrumentation data relative to the relocation event are conceptually compatible in most respects with a "thermal sequence" consisting of the following three stages:

Stage I: A transient heat-up and remelting interval within the ceramic agglomerate, the onset of which is difficult to define but probably began shortly after the agglomerate formed from the draining and refreezing of core material in the vicinity of the water-steam interface and lasted for, say, less than 1 hour.

Stage II: A subsequent but relatively short quasi-steady period of from several seconds to perhaps a few minutes in duration in which most of the dense agglomerate was molten and transferring decay heat by natural convection to the surrounding water through a protective crust*. The crust can be thought of as a hemispherical ceramic "cup or crucible", covered by a thin crust cover, that contained the remelted agglomerate (ceramic) material.

Stage III: The actual fuel relocation event followed the collapse of the thin crust cover under the weight of the overlying rubble bed. The relocation was accompanied by steam generation (and a concomitant increase in primary system pressure) as a result of intermittent contact between satur-

*This is not meant to imply that the period of time during which a large fraction of the agglomerate was molten was short, but, instead, that the water surrounding the agglomerate felt the presence of its molten interior for a period of time that was negligible on the scale of the heat-up period (Stage I).

ated water trapped in the interstices of the rubble bed and the ceramic melt and at a rate controlled by either the peak nucleate boiling heat flux or the dryout heat flux. The rubble bed displaced the ceramic melt, the melt material flowed downward over a period of about one minute through the intact core structure as a hot liquid jet in a continuum of subcooled water with little net steam generation, and, because of hydrodynamic fragmentation, reached the lower plenum as a stream of solidified drops of high coolability.

In the present report we consider this basic mechanistic picture in some detail. Our treatment of Stage I is simply aimed at showing that during this initial period very little heat was transferred from the impervious solid ceramic in the central core region to the surrounding water. That is, very little steam entered the rubble bed above the ceramic agglomerate as a result of boiling off its surfaces. The absence of such steam production would allow the water injected into the core at 200 min to gradually enter the overlying rubble bed and quench it. The occurrence of quenching is consistent with the mechanism postulated for the primary system pressure increase during Stage III. We conclude from our analysis of Stage II that the relocation event must have occurred just before the molten ceramic region within the interior of the hemispherical agglomerate reached its steady-state configuration. Accordingly, the water surrounding the ceramic agglomerate and, more importantly, in the interstices of the rubble bed did not "feel" the decay heat generated within this region until the rubble bed penetrated the upper crust and entered the molten interior of the consolidated region. The study of Stage III includes an estimation of the size of the particle fragments in the lower plenum, the thermal interaction between molten core material and coolant water, and the inference that the water in the core below the rubble bed was subcooled when the fuel relocated to the lower plenum. The main implications of this study for future work, including core bore sampling operations, are outlined in Section 5, which concludes the present report.

2.0 HEAT-UP PERIOD

It is of interest to determine whether during Stage I the temperature gradient just beneath the surface of the ceramic agglomerate was too small to produce any significant rates of steam production at the surface. Clearly, the temperature at the outer surface of the ceramic agglomerate and, therefore, the heat flux at the surface are determined to some extent by the mechanism of heat removal in the surrounding water. The assumption of constant temperature at the surface, however, is sufficient for estimating the maximum rate of heat loss or, equivalently, steam production. This leads to the model depicted in Figure 2-1 of the temperature profile within the upper crust of the ceramic agglomerate, that separates its molten interior from the rubble resting on top of the crust. The upper crust shown in the figure is what remains of the original upper portion of the ceramic agglomerate; it is gradually being eroded (melted) from the inside by the convecting and growing molten interior.

The heat flux q_u convected upward from the molten interior is approximately 10^6 W m^{-2} (see Section 3). The variation in temperature above the melt front occurs over a boundary layer thickness δ of [4]

$$\delta = \frac{\alpha}{U} \tag{2-1}$$

where α is the thermal diffusivity of the crust material and U is the velocity of melting:

$$U = \frac{q_u}{[h_{fs} + c\,(T_{mp} - T)]\,\rho} \tag{2-2}$$

In the above equation h_{fs}, ρ, c and T_{mp} are the latent heat of melting, density, heat capacity, and melting temperature of the ceramic agglomerate respectively. If one has independent knowledge of the temperature T in the crust far from the melting boundary, U can be calculated. A preliminary estimate based on a 45 min heat-up period from the water saturation

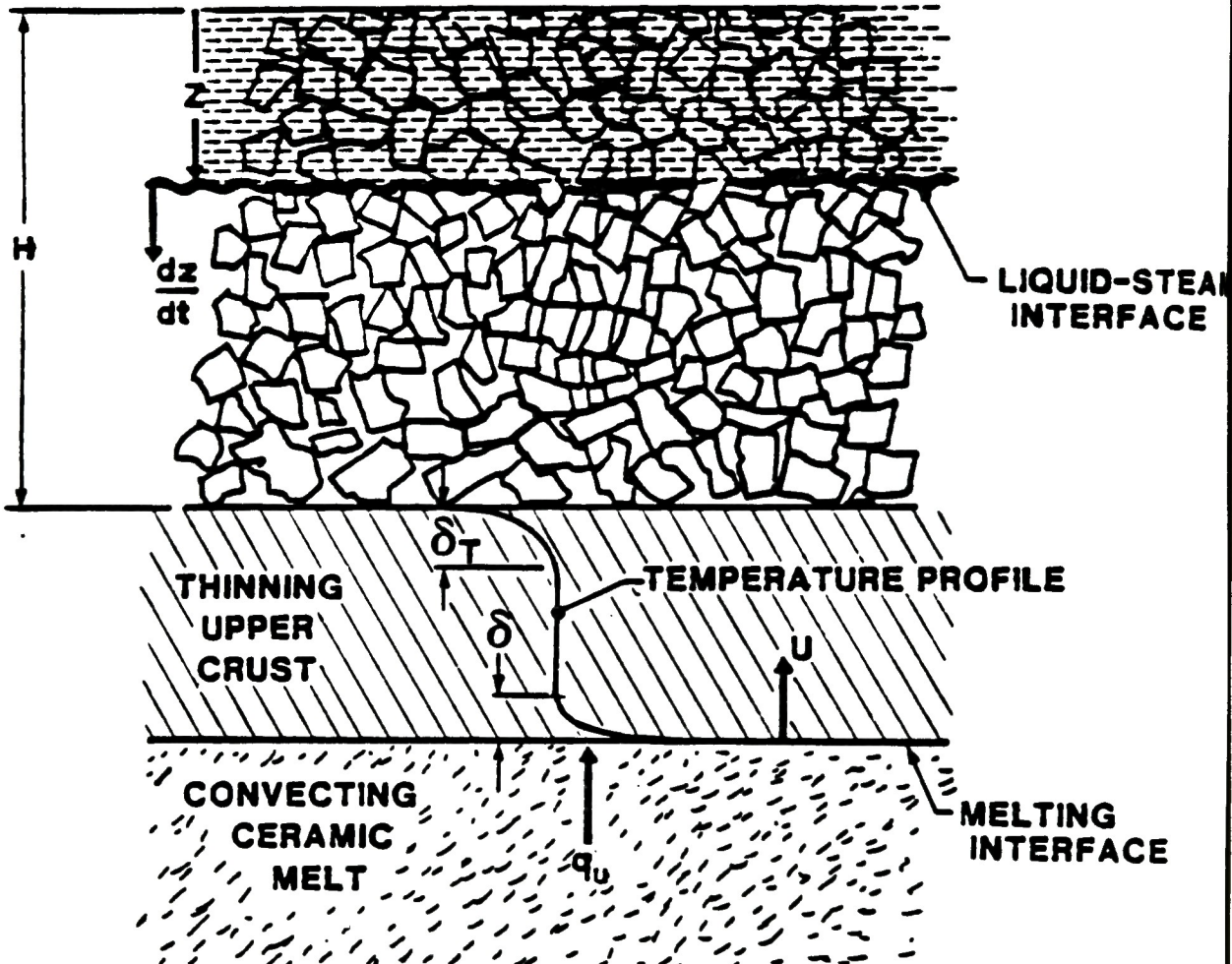

Figure 2-1 Schematic representation of core heatup stage, illustrating quenching of the rubble bed and the temperature profile in the upper crust.

temperature is T = 1600 K. This value of T, together with the estimates h_{fs} = 2.8 x 10^5 J kg^{-1}, ρ = 10^4 kg m^{-3}, c = 430 J kg^{-1} K^{-1}, T_{mp} = 2800 k, and α = 7 x 10^{-7} m^2 S^{-1}, indicates from Equations (2-1) and (2-2) that U and δ are of the order 0.1 mm s^{-1} and 6 mm, respectively. It follows from these numerical results that the thermal boundary layer surrounding the molten zone was very thin on the scale of the dimension(s) of the crust thickness during the heat-up period, as illustrated in Figure 2-1. In other words, the heat generated in the molten interior was not felt by the surrounding water until the moving melt boundary encountered the thermal layer that moved inward from the surface. The merging of the two thermal waves corresponds to the attainment of a steady-state ceramic melt-pool configuration. An examination of the steady-state ceramic pool will be presented in the next section, from which we conclude that core relocation probably occurred before a steady-state ceramic pool was achieved.

It is clear from the discussion in the foregoing that during Stage I the heat transferred to the water surrounding the central consolidated region was generated only in a thin layer of instantaneous thickness δ_T just beneath the surface (see Figure 2-1). Thus the maximum possible heat flux q off the surface of the agglomerate is equivalent to that at the isothermal surface of a semi-infinite solid with internal volumetric heat generation Q; namely [4]

$$q = 2Q\,(\alpha\, t/\pi)^{1/2} \qquad (2\text{-}3)$$

Noting that the decay heat rate Q = 1.5 x 10^6 W m^{-3} [5] and setting the time t = 2.7 x 10^3 s (45 min) provides a surface heat flux of 7.4 x 10^4 W m^{-2}. This may be compared to the predicted heat flux off the top of the rubble bed, as given by

$$q = QH\,(1 - \varepsilon), \qquad (2\text{-}4)$$

where H is the height of the rubble bed (See Figure 2-1) and ε is its porosity. Equation (2-4) with H = 0.93 m and ε = 0.54 [6] gives q = 6.4 x 10^5 W m^{-2}. Hence the steam generated at the upper surface of the consolidated region after 45 min of internal heating is a factor of 10 less than

that generated within the rubble bed overlying the consolidated region. We conclude that during Stage I the steam generated at the top of the consolidated region did not interfere with the quenching of the overlying debris bed by the coolant injected into the primary system at 174 min and after 200 min into the accident.

The dryout heat flux q_{dry} for the rubble bed itself can be estimated with the model of Lipinski [7] in the turbulent flow limit:

$$q_{dry} = \frac{h_{fg}\left[\rho_g\,(\rho_w - \rho_g)\,gn\right]^{1/2}}{\left[1 + (\rho_g/\rho_w)^{1/4}\right]^2} \tag{2-5}$$

where n is the bed permeability

$$n = \frac{d}{1.75}\,\frac{\varepsilon^3}{1-\varepsilon} \tag{2-6}$$

d is the average particle diameter, ρ_g and ρ_w are the density of the steam and water, respectively, and h_{fg} is the latent heat of evaporation of water. As a result of the sampling of the upper debris bed and particle size distribution analysis, the best estimate of the average particle size is d = 0.9 mm [6,8]. Note that for TMI conditions the laminar contribution to dryout can be ignored for $d \gtrsim 0.38$ mm. Taking ρ_g = 55.4 kg m^{-3}, ρ_w = 688 kg m^{-3} and $h_{fg} = 1.32 \times 10^6$ J kg^{-1}, corresponding to a system pressure of 10 MPa, we predict

$$q_{dry} = 4.4 \times 10^6 \text{ W m}^{-2} \tag{2-7}$$

The condition for dryout, namely

$$q_{dry} < QH\,(1-\varepsilon) = 6.4 \times 10^5 \text{ W m}^{-2}, \tag{2-8}$$

is <u>not</u> satisfied. Thus the water injected into the core ultimately resulted in quenching of the rubble bed. This may have been a relatively long-term

process, with water gradually penetrating the interior of the rubble bed from the core periphery. Accordingly, it is of interest to examine the depth to which the water penetrated the rubble bed before core relocation occurred, assuming that water first entered the top of the rubble bed immediately after the high pressure injection system was turned on at 200 min.

Based on the concepts that (i) the propagation of the quench (water) front is controlled by local flooding or dryout and (ii) the hot debris particles are completely quenched and cooled to the water saturation temperature at the water front, Cho et al. [9] and Ginsberg et al. [10] developed a differential expression for the location of the front z, measured from the top of the rubble bed (see Figure 2-1). This expression, as modified by Kuan [6] to account for the effect of decay heating, is

$$\rho c\,(1-\epsilon)\,\Delta T\,\frac{dz}{dt} = q_{dry} - Q(1-\epsilon)\,(H-z) \qquad (2\text{-}9)$$

here ΔT is the initial temperature of the bed relative to the water saturation temperature. Integrating Equation (2-9) from $z = 0$ at $t = 0$ and solving the result for z, we get

$$z = \left[\frac{q_{dry}}{Q(1-\epsilon)} - H\right] \cdot \left(e^{\frac{Qt}{\rho c \Delta T}} - 1\right) \qquad (2\text{-}10)$$

Using $\Delta T = 1500$ k, we estimate from Equation (2-10) that the water quenches the entire 0.92 -m deep rubble bed in the time interval between coolant injection at 200 min and core relocation at 224 min. This prediction suggests that the collapse of the upper crust could readily bring the interstitial water in the rubble bed into direct contact with the molten interior. We will return to this issue later on.

Kuan [6] has recently considered the problem of dryout in the rubble bed, using a more conservative dryout model which is essentially equivalent to Equation (2-5) with the denominator replaced by $[1 + (\rho_g/\rho_w)^{1/6}]^3$. This expression results in a factor of two reduction in q_{dry} relative to that

appearing in Equation (2-7). The implication of Kuan's result is that the argument for little thermal communication between the consolidated region and the rubble bed during the heat-up period is critical to the prediction of a quenched rubble bed.

3.0 STEADY STATE MOLTEN CERAMIC REGIME

The core-boring operations have provided sufficient data to estimate the end-state geometry of the core region. As already mentioned, a near hemispherically shaped region of previously molten fuel has been identified. Assuming that this was the shape of the molten region during the heat-up period, we consider the steady-state molten-ceramic-pool model illustrated in Figure 3-1. While we do not believe that the molten interior of the consolidated region reached a true steady-state before core failure, useful by-products of this model are the identification of a plausible mechanism for the core relocation event and a rough estimate of the temperature (superheat) of the molten region.

The heat produced by radioactivity within the interior of the molten region is equal to the heat loss rate to the bounding crust surfaces. Owing to the presence of the crust, the steady-state molten region supplies a constant heat flux to the interior surface of the crust at all times. While the heat flux is considered constant for each circumferential element of the lower hemispherical crust, it may vary with angular position θ from the center line (See Figure 3-1). To estimate the local heat fluxes requires heat transfer correlations for natural convection within the melt at temperatures above 2800 K. While this information is presently not available, it is felt that correlations obtained with low temperature water pools are adequate for scoping or preliminary safety assessments.

Unfortunately, most experimental studies of thermal convection in water layers with volumetric energy generation have dealt essentially with two-dimensional systems. To date, no experimentally derived heat transfer correlations for both the upper and lower surfaces of a hemispherical cavity are available. We will assume here that the correlations reported by Jahn and Reineke [11] and Mayinger et. al. [12] for free convection within a semicircular cavity of radius R are applicable to a hemispherical cavity having the same radius. Gabor et. al [13] reported an empirical correlation for the average <u>downward</u> heat flux from an internally heated hemispherical pool. The downward heat flux rate measured in the three studies are in

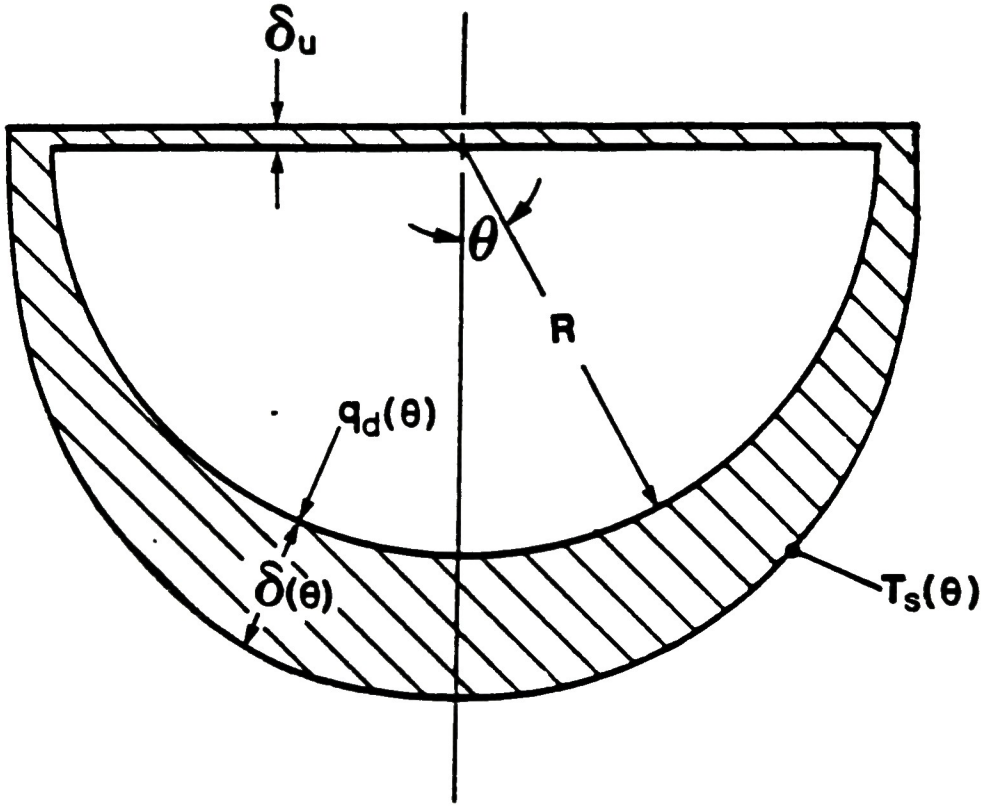

Figure 3-1 Natural-convection model of the molten region within the TMI-2 core.

reasonable agreement, suggesting, perhaps, that the application of the correlations for a semicircular cavity to the hemispherical cavity is acceptable. It should be noted that part of Reference [12] is devoted to the presentation of numerical computations of turbulent natural convection within heat generating fluids. The numerical study of the hemispherical cavity results in an average heat transfer coefficient to the lower surface that is slightly larger than that to the upper surface. However, according to Kulacki [14], the authors' model of turbulence is adapted from notions about turbulent shear flow in forced convection, and thus its application to free convection, where there is no mean shear, should be regarded with caution.

Based on the work reported in [12] with the semicircular, two dimensional test cell, the following heat transfer correlations are employed in our study of the hemispherical molten zone:

$$\frac{q_u R}{k\Delta T} = 0.36\ Ra^{0.23} \tag{3-1}$$

for the upward heat flux, q_u, to the pool's crust cover,

and

$$\frac{\bar{q}_d R}{k\Delta T} = 0.54\ Ra^{0.20} \tag{3-2}$$

for the average downward heat flux, $\bar{q}_d$, to the lower crust surface. In the above correlations ΔT is the pool temperature T relative to its melting temperature T_{mp}, k is the thermal conductivity of the melt, R is the radius of the molten zone and Ra is the Rayleigh number for a heat generating fluid:

$$Ra = \frac{g\beta QR^5}{\alpha\nu k} \tag{3-3}$$

where β, α, ν, are the coefficient of volumetric expansion, thermal diffusivity and kinematic viscosity of the molten ceramic material, respectively, g is the gravitational acceleration, and Q is the volumetric heat generation rate.

The overall energy balance that equates the heat production rate to the heat loss rate is

$$\frac{1}{2} \cdot \frac{4}{3} \pi R^3 Q = \pi R^2 q_u + \frac{1}{2} \cdot 4\pi R^2 \bar{q}_d \tag{3-4}$$

Substituting Equations (3-1) and (3-2) into Equation (3-4) to eliminate q_u and q_d, we get, after solving for ΔT

$$\Delta T = \frac{2}{3} \cdot \frac{QR^2}{k} \left(0.36\ Ra^{0.23} + 1.08\ Ra^{0.18}\right)^{-1.0} \tag{3-5}$$

The thermal properties of the ceramic melt are taken to be: $k = 3\ W\ m^{-1}\ K^{-1}$, $\alpha = 7 \times 10^{-7}\ m^2\ s^{-1}$, $\nu = 6 \times 10^{-7}\ m^2\ s^{-1}$, and $\beta = 10^{-4}\ K^{-1}$. The radius assumed for the hemispherical ceramic melt region is $R = 1.25\ m$*, and the decay heat rate within the melt $Q = 1.5 \times 10^6\ W\ m^{-3}$ (see Reference [5]). These estimates result in a melt region Rayleigh number

$$Ra = 3.56 \times 10^{15} \tag{3-6}$$

and a pool superheat

$$\Delta T = T - T_{mp} = 256\ K \tag{3-7}$$

where T_{mp} is the melting point of the ceramic material ($\sim$ 2800K). Substituting these values into Equation (3-1), we obtain the heat flux impinging on the inner surface of the crust cover; namely

$$q_u = 8.35 \times 10^5\ W\ m^{-2} \tag{3-8}$$

---

*R is the radius of a hemisphere having approximately the same volume as the consolidated region as determined from the core boring operations [16].

The average downward heat flux to the lower, hemispherical crust surface is, from Equation (3-2)

$$\bar{q}_d = 2.09 \times 10^5 \text{ W m}^{-2} \tag{3-9}$$

The experimental study of Jahn and Reineke [11] has shown that the local heat flux varies considerably along the lower boundary of the convection cavity. The local heat flux $q_d(\theta)$ as a function of angular position from the center line is presented in Figure 7 of Reference [11] for the Rayleigh number range 10^7 - 10^{11}. Assuming that the functional relation $q_d(\theta)$ illustrated in this figure is valid in the large Rayleigh number regime of interest here, namely Ra $\sim 10^{16}$, the local thickness of the crust $\delta(\theta)$ can be estimated by solving the one-dimensional conduction equation for heat flow within the crust. Conduction theory yields the following quadratic equation for the crust thickness $\delta(\theta)$:

$$\frac{Q\delta(\theta)^2}{2k} + \frac{q_d(\theta)\,\delta}{k} = T_{mp} - T_s(\theta) \tag{3-10}$$

where $T_s(\theta)$ is the local temperature of the outer surface of the crust (see Figure 3-1).

The heat loss from the outer surface is mainly due to thermal radiation, as film boiling is the expected "heat-transfer regime" on the lower boundary of the consolidated region. Back radiation from the water surrounding the molten core is negligible; so that, by equating the sum of the heat flux from the molten interior and that generated within the lower crust with the radiation heat loss gives

$$q_d(\theta) + Q\delta(\theta) = e\sigma T_s^4(\theta) \tag{3-11}$$

where e is the emissivity of the surface of the ceramic crust (e = 0.8 [15]) and σ_B is the Stefan-Boltzman constant (5.6×10^{-8} W m^{-2} K^{-4}). Equations (3-10) and (3-11) represent an algabraic system for the two unknown quantities $T_s(\theta)$ and $\delta(\theta)$.

Combining the information in Figure 7 of Reference [11] with Equations (3-10) and (3-11), provides predicted values of the functions $T_s(\theta)$ and $\delta(\theta)$ which are plotted in Figure 3-2. It was pointed out in the previous section that water penetrated the rubble bed and was in direct contact with the upper crust sometime during Stage I. On this upward facing boundary conditions were more favorable for nucleate boiling than for film boiling. Clearly, the assumption of nucleate boiling results in an upper bound estimate of the thickness of the upper crust. The appropriate boundary condition in this case is one of constant surface temperature equal to the system saturation temperature T_{sat}. Taking the system pressure to be 10 MPa at the inception of core relocation yields a saturation temperature T_{sat} = 584 K. Equation (3-10) with $T_s(\theta) = T_{sat}$ and $q_d(\theta) = q_u$ then provides an estimate of the crust cover thickness, namely

$$\delta_u = 7.9 \text{ mm} \qquad (3\text{-}12)$$

Had we assumed that the upper crust supported film boiling our estimate of the crust cover thickness becomes δ_u = 2.6 mm.

Based on the crust thickness estimates presented in Figure 3-2 and the fact that the lower hemispherical crust is supported from below by an intact fuel pin matrix, one can conclude that the bottom of the crust cup was not a likely path for fuel escape from the TMI core. On the other hand, the upper crust is relatively thin and probably could not have supported the mass of solid, loose debris believed to have been resting on top of the consolidated region. According to the stress analysis reported by Kuan [5], the upper crust would have collapsed under the weight of the debris if its thickness was less than about 2.5 cm, which is much thicker than our estimate based on steady state. Thus it is conceivable that the loose debris fell through the surface of the molten region before the region achieved its steady-state configuration. This is consistent with our previous assumption of negligible thermal interaction between the consolidated region and the surrounding water, in particular the water within the overlying rubble bed.

Perhaps the sudden relocation of core material at 224 min can be explained by molten ceramic flowing over the edge of the pool as it is

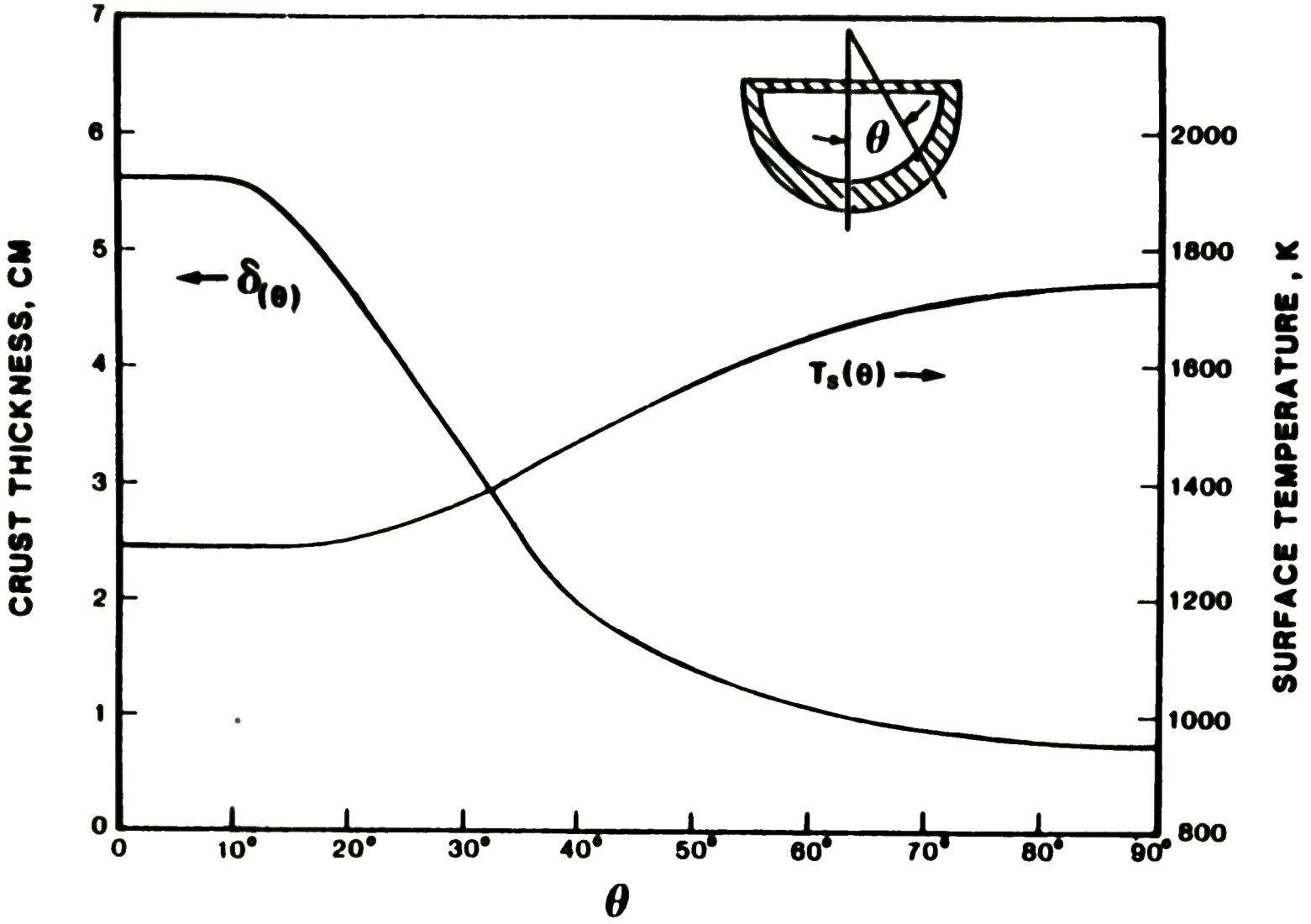

Figure 3-2 Predicted variation of crust crucible thickness and surface temperature with angular position.

displaced by settling debris. It should be noted from Figure 3-2 that the crust is fairly thin at the edge of the hemisphere, i.e., at $\theta > 60°$. Simultaneous failure of the crust cover and a localized edge failure could explain why the melt migration path was limited to a small cross section of the core periphery, as revealed by the core boring data [16]. Moreover, the existing "sinkhole" in the rubble bed [2,16] is nicely explained by the crust failure mechanism of core relocation. A proposed history of the relocation event is illustrated in Figure 3-3.

While our calculations in support of the crust failure mechanism have been made only for a specific set of physical property values, ceramic pool dimension and heat-transfer correlations, it may be shown that the physical picture presented in Figure 3-3 is rather insensitive to uncertainties in these quantities. This is because the thicknesses of the upper and lower crusts relative to each other are of greatest physical interest rather than their absolute magnitudes. That is, within the ranges of uncertainty of the input values, the conclusion that the upper crust is thin and unstable under the weight of the debris while the lower crust is thick and well supported remains unchanged.

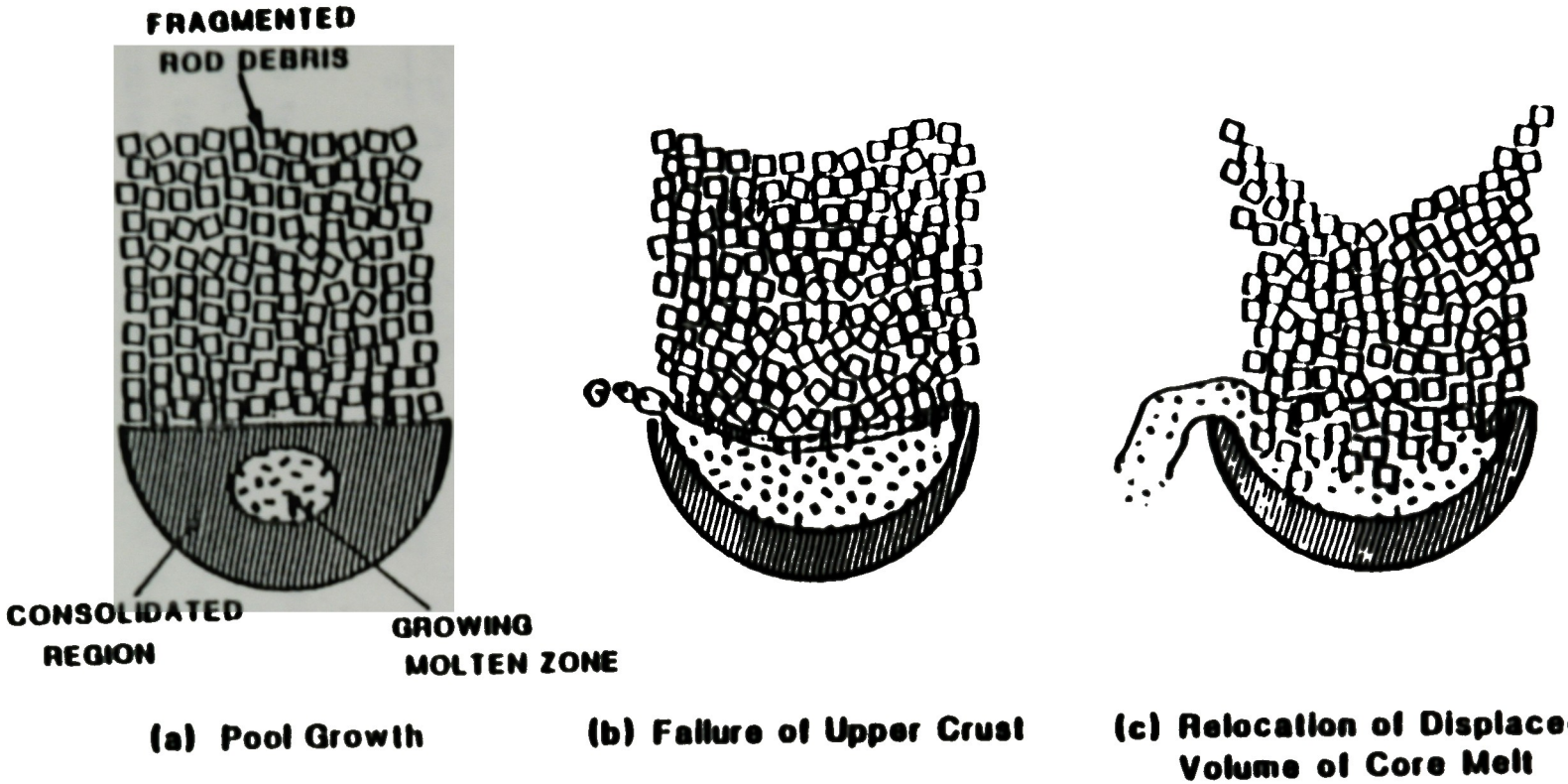

Figure 3-3 Postulated sequence of events leading to core material relocation.

4.0 CORE RELOCATION

4.1 Duration of Relocation Event and Steam Generation

The timing of the relocation event, based on the sequence proposed in the foregoing (Figure 3-3), may depend on the rate of settling of the debris. This is a difficult process to treat mathematically. The motion of loose debris is whimsical and bewildering and defies any rational treatment from first principles. One, however, can always obtain an indication of the maximum settling rate by equating the drag exerted on the particles of a rigid debris bed by the molten ceramic with the mass of the bed. If a rigid mass of particles of size d settles downward in a vertical vessel containing a fluid of density ρ, the drag force acting on the particle mass per unit area of bed is [17]

$$F = \frac{2c_f\rho}{d}\left(\frac{1-\epsilon}{\epsilon^3}\right) z \left(\frac{dz}{dt}\right)^2 \qquad (4\text{-}1)$$

where ϵ is the porosity of the rubble bed, c_f is the friction factor for flow in porous media, and z and dz/dt are the instantaneous depth of submergence and settling velocity of the debris pile, respectively. The terminal behavior of the settling debris can now be determined by balancing the gravitational and drag forces:

$$\frac{2c_f\rho}{d}\left(\frac{1-\epsilon}{\epsilon^3}\right) z \left(\frac{dz}{dt}\right)^2 = (H-z)\,(1-\epsilon)\,\rho g \qquad (4\text{-}2)$$

where H is the total length of the rubble bed in the direction of motion. Note that in writing Equation (4-2) we have assumed that the density of the melt is identical to that of the rubble bed material, or, equivalently, that the rubble bed particles are neutral density particles when submerged in the ceramic pool.

Assuming turbulent settling behavior, such that c_f is approximately constant and equal to 0.88, and integrating Equation (4-2), we obtain the inverted solution

$$t = H\left(\frac{2c_f}{dg\epsilon^3}\right)^{1/2}\left[\frac{\pi}{2} - \tan^{-1}\left(\frac{H-z}{z}\right)^{1/2} - \left(\frac{z}{H}\cdot\frac{H-z}{H}\right)^{1/2}\right] \qquad (4\text{-}3)$$

The core sampling data and analysis work indicates an initial height of the upper rubble bed of H = 0.93 m, a bed porosity of ϵ = 0.54, and an average debris particle size d = 0.9 mm [6,8]. Based on these estimates and Equation (4-3), the time for the debris to settle a vertical distance of, say, z = 0.5 m into the ceramic pool is 12 sec. A value of core relocation time of approximately 60 sec is indicated from the plant instrumentation data. One can interpret this discrepancy as an indication that laminar flow and solidification within the interstices of the debris were operative as the debris settled into the ceramic region. In fact, as shown below, solidification can quickly seal all the fluid paths within the submerged portion of the debris configuration.

The hydraulic radius R_h of the settling debris is taken to be equivalent to that of a packed bed [18]:

$$R = \frac{\epsilon d}{6(1-\epsilon)} \qquad (4\text{-}4)$$

It is reasonable to suppose that once the thickness δ of the freeze layer on a representative debris particle grows to R_h, the leading edge of the settling debris is closed to the additional penetration of melt material. Since R_h is not an appreciable fraction of the particle radius, the crust growth process is well represented by a one-dimensional treatment. Assuming quasi-steady heat transport rates in both the particle and its crust envelope, the instantaneous crust thickness δ and particle temperature, $T_p(t)$, can be expressed by the differential equations

$$\frac{d\delta}{dt} = \frac{k\ (T_{mp} - T_p)}{\rho h_{fs}\ \delta} \tag{4-5}$$

and

$$\frac{1}{6}\ doc\ \frac{dT_p}{dt} = \frac{k\ (T_{mp} - T_p)}{\delta} \tag{4-6}$$

Eliminating T_p between these equations and integrating the result from $\delta = 0$ at $t = 0$ to $\delta = R_h$ at $t = t_{fr}$, the time to freeze the settling debris shut, gives

$$\frac{36\alpha t_{fr}}{d^2} = -\frac{\epsilon}{1-\epsilon} - \frac{c\ (T_{mp} - T_{p,o})}{h_{fs}} \cdot \ln\left[1 - \frac{\epsilon}{1-\epsilon} \cdot \frac{h_{fs}}{c\ (T_{mp} - T_{p,o})}\right] \tag{4-7}$$

where $T_{p,o}$ is the temperature of the overlying rubble at the instant the supporting crust fails. The quasi-steady solidification time may considerably exceed the actual solidification time. Nevertheless, our experience with problems of this type indicates that Equation (4-7) allows us to estimate the order of magnitude of t_{fr}. The debris enters the ceramic pool at the water saturation temperature, $T_{p,o} = T_{sat} = 584K$ (See Section 2). This leads to the estimate

$$t_{fr} = 0.01\ s \tag{4-8}$$

The distance the debris settles during this time is, approximately,

$$z = 1/2\ g\ t_{fr}^2 = 0.049\ m \tag{4-9}$$

and the settling velocity is

$$\frac{dz}{dt} = g\ t_{fr} = 0.098\ m\ s^{-1} \tag{4-10}$$

which is too low to cause a limitation to crust growth due to forced convection (ceramic melt superheat $T-T_{mp}$) within the interstices of the debris bed. A sufficient condition for the neglect of forced convection is

$$\frac{R_h\ h\ (T - T_{mp})}{k\ (T_{mp} - T_{p,o})} << 1 \qquad (4\text{-}11)$$

For the settling (or superficial) velocity given by Equation (4-10), we obtain the heat-transfer coefficient $h = 5.4 \times 10^4$ J s^{-1} m^{-2}, from the heat-transfer correlation for flow within packed beds of Hougen and Marshall [19]:

$$h = 0.58\ \frac{k}{d}\left(\frac{\dot{z}d}{\nu}\right)^{2/3} \qquad (4\text{-}12)$$

Since $T-T_{mp} = 256$ k, from Equation (3-7), the left-hand side of Equation (4-11) is at most 0.36. This result shows that forced-convection corrections to freezing are not too important.

The results obtained above show that the ceramic melt will not pass through the rubble bed as it settles into the hemispherical cavity. Instead the melt will be forced toward the cavity wall and up some annular region between the wall and the settling rubble bed. Of course, an estimate of the dimensions of such a flow path is not possible. However, it is reasonable to presume that the inability of the melt to pass upward through the rubble bed as well as the tendency of the particles to bind during settling will extend the relocation time beyond the 12 s predicted with Equation (4-3). Alternatively, the water that entered the debris bed during the heat-up stage could have limited the rate at which relocation occurred, and this is the subject of the remainder of this section.

It is important to recognize that the debris, during the process of settling into the ceramic melt, will force the water in the interstices into contact with the surfaces of the molten ceramic region. Such intimate, forced contact conditions may be capable of causing the water boiling rate

at the surface to increase dramatically and approach the peak or "critical" nucleate boiling rate. In fact, it is interesting to speculate that the maximum rate at which water can be removed from the surface of the ceramic melt via boiling controls the rate at which the rubble displaces the ceramic melt. It seems likely that the molten ceramic will form a thin crust cover upon contact with water. This cover is presumed to temporarily halt the downward movement of the rubble bed. The water recedes from the crust into the now stationary rubble bed at a rate determined by boiling. The crust cover heats up, weakens, and fails under the weight of the rubble, and once again the settling debris drives the interstitial water into contact with the ceramic melt and the process repeats itself. We can test the utility of this conceptual picture by asking the following questions: Is the observed primary system pressurization rate consistent with nucleate boiling off the top of the molten ceramic region?, and is the boiling rate consistent with the time scale of the relocation event as inferred from the plant instrumentation?

We illustrate a procedure for answering these questions here using the Zuber [20] flat plate critical heat flux expression to estimate the boiling rate off the surface of the exposed melt, namely,

$$q_{crit} = 0.14\, h_{fg}\, \rho_g \left[\frac{\sigma g\,(\rho_w-\rho_g)}{\rho_g^2}\right]^{1/4} \qquad (4\text{-}13)$$

For the pressure condition of P = 10 MPa during core relocation, the latent heat of evaporation $h_{fg} = 1.32 \times 10^6$ J kg^{-1}, the steam density ρ_g = 55.36 kg m^{-3}, the water density ρ_w = 688.0 kg m^{-3}, and the water surface tension σ = 0.0119 N m^{-1}. The critical heat flux is calculated to be

$$q_{crit} = 4.03 \times 10^6 \text{ W m}^{-2} \qquad (4\text{-}14)$$

The corresponding "critical" mass rate of steam production at the top of the hemispherical melt region of radius R is

$$\dot{m}_{crit} = \frac{\pi R^2 q_{crit}}{h_{fg}} = 15 \text{ kg S}^{-1} \tag{4-15}$$

Steam is also added to the primary system by boiling within the overlying rubble bed at a rate given approximately by

$$\dot{m}_b = \frac{\pi R^2 QH(1-\varepsilon)}{h_{fg}} = 2.4 \text{ kg S}^{-1} \tag{4-16}$$

During the core relocation period steam is lost from the primary system through the pressurizer relief valve. The pressurizer fluid level history suggests that the exhaust flow was pure steam from core reflood (174 minutes) to 246 minutes [21]. The exhaust flow rate of steam through the valve, $\dot{m}_{val}$, can be evaluated via the well-known expression for the choked flow of an ideal gas:

$$\dot{m}_{val} = C_D A_{val} P \left[\frac{\gamma}{R_g T}\left(\frac{2}{\gamma+1}\right)^{\frac{\gamma+1}{\gamma-1}}\right]^{1/2} \tag{4-17}$$

where R_g is the gas constant for steam and P,T are the primary system pressure and temperature. With a discharge coefficient $C_D = 0.78$, valve flow area $A_{val} = 8.71 \times 10^{-4}$ m^{-3} [21], and a ratio of specific heats for steam $\gamma = 1.27$, we estimate using Equation (4-17)

$$\dot{m}_{val} = 8.7 \text{ kg S}^{-1} \tag{4-18}$$

It is assumed that no steam is produced from the largely intact fuel rods, owing to the sub-cooling of the water around these rods (see next section). The net steam production rate, $\dot{m}_{net}$, during core relocation is, then,

$$\dot{m}_{net} = \dot{m}_{crit} + \dot{m}_b - \dot{m}_{val} = 8.7 \text{ kg S}^{-1} \tag{4-19}$$

The net steam production rate can be inferred from the measured system pressurization data and the relation

$$\dot{m}_{net} = \frac{V}{R_g T}\frac{dP}{dt} \tag{4-20}$$

where V is the volume for steam expansion in the primary system. Interpretation of the TMI-2 data base suggests a primary system pressure response of approximately $dP/dt \sim 2.2 \times 10^4$ Pa S^{-1} [22] and a system void volume $V \sim 116$ m^3 [6]. Using these estimate in Equation (4-20) it follows that the "measured" net steaming rate at core relocation is approximately 9.5 kg m^{-3}, which is remarkably close to that predicted on the basis that steam generation during core relocation was caused mainly by the interaction of water in the interstices of the debris bed with the ceramic melt as the debris displaced the melt material.

Finally, it is of interest to determine whether the observed core relocation time is consistent with a nucleate boiling limitation on the rate at which the rubble bed displaced the ceramic melt. According to this idea, the volume of interstitial water boiled away at the melt surface during the core relocation period t is equal to the volume of ceramic melt displaced, or

$$\pi R^2 q_{crit}\, t/(h_{fg}\rho_w) = \frac{2}{3}\pi R^3 \varepsilon \tag{4-21}$$

Solving for t and inserting the present numerical estimates for q_{crit} and R, we get

$$t = \frac{2}{3}\frac{R\rho_w h_{fg}\,\varepsilon}{q_{crit}} = 101 \text{ S} \tag{4-22}$$

which compares very well with the core material relocation time of approximately 80 s, as inferred from the source range monitor response [22].

It may be useful to know that a successful boiling limitation argument for the rate of steam generation and rubble bed collapse can be based on a dryout mechanism within the debris bed instead of peak nucleate boiling, as the two corresponding heat fluxes are almost identical [compare Equation (2-7) with Equation (4-14)].

4.2 The Breakup and Quench of the Core Material Stream

The initial contact mode between molten core material and water has been postulated in the foregoing to come about by the collapse of the rubble bed into the molten zone. It was demonstrated that this melt/water interaction could have been entirely responsible for the observed primary system pressure response. Hence there is the implication that little or no net steam production occurred by the downward draining of the liquified core material through the lower region of the fuel elements and the lower plenum region. Presumably the stream (or jet) of molten core material passed through highly subcooled water on its way to the bottom of the reactor vessel. Here we attempt to demonstrate this by assuming that the water below the molten region of the core was nearly saturated. The unreasonableness of this assumption then follows from the fact that the predicted jet breakup rate and simultaneous steam generation rate in saturated water is much too high to account for the observed system pressure response. Moreover, there is both theoretical and indirect experimental evidence that hot, molten pour streams will penetrate many more jet diameters in saturated water without substantial breakup than in subcooled water. The character of the debris layer which collected on the bottom of the TMI vessel is shown below to be more consistent with a melt stream/subcooled water interaction.

It should be mentioned at the outset that it is difficult to provide accurate predictions of the jet breakup rate by the mechanical action of the ambient fluid. Even in the simplest case of a liquid jet moving through a gaseous atmosphere, an early appeal to experiment is necessary to determine the unknown constant(s) of proportionality that enters jet stability theory. Moreover, while considerable experimental and theoretical work has been reported on the rate of liquid jet breakup in air, there is a lack of quantitative information on breakup rates of hot liquid jets in boiling

liquid media. Here we will pursue a simple semi-empirical approach to the problem of the breakup of molten jets in boiling water. As is usual in jet stability theory, the process of droplet formation at the surface of the molten-core material jet is interpreted to be due to the breaking of infinitesimal amplitude capillary waves (ripples). As we shall see below, the capillary wavelength is very small compared with both the diameter of the jet and the spacing between fuel rods so that the effects of jet curvature and rod surfaces on jet stability can be ignored.

From Lamb [23] we have the growth of a two-dimensional wave of amplitude η having initial wave length λ (see Figure 4-1):

$$\frac{d\eta}{dt} = m\eta \tag{4-23}$$

where

$$m^2 = \frac{\rho_j \rho_\infty}{(\rho_j + \rho_\infty)^2} k^2 u_j^2 - \frac{\sigma_j}{\rho_j + \rho_\infty} k^3 \tag{4-24}$$

In the above equation for the wave growth constant m, k is the wave number ($k = 2\pi/\lambda$), u_j is the jet velocity, σ_j is the surface tension of the jet material, and ρ_j and ρ_∞ are the densities of the molten jet and the surrounding fluid (water or steam), respectively. The following idealized jet breakup mechanism will be assumed. The most rapidly growing capillary wave, which is found when m as a function of k in Equation (4-24) exhibits a maximum (m_{max}), is detached as a ridge of liquid of diameter comparable with $\lambda/2$ and width $w = \pi d_j$, where d_j is the diameter of the jet. Thus the most rapidly growing capillary wave will detach from the jet surface after a characteristic growth time [see Equation (4-23)].

$$t \sim \frac{1}{m_{max}} = \frac{\sqrt{27}}{2} \frac{(\rho_\infty + \rho_j)^2}{(\rho_\infty \rho_j)^{3/2}} \cdot \frac{\sigma_j}{u_j^3} \tag{4-25}$$

in the form of a ridge of mass

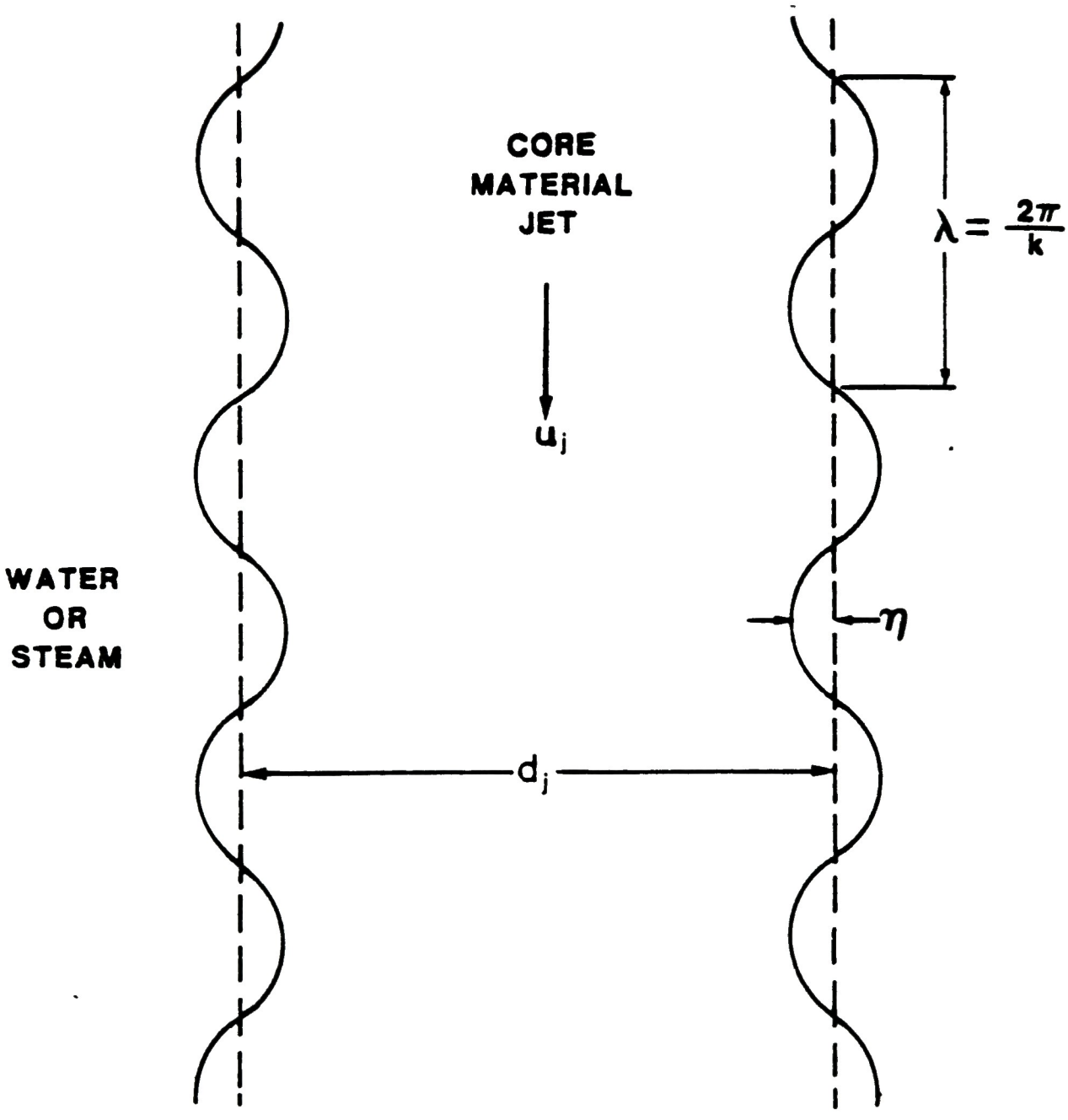

Figure 4-1 Jet stability model.

$$= \pi \left(\frac{\lambda_{max}}{4}\right)^2 w_{o_j} \tag{4-26}$$

where

$$\lambda_{max} = \frac{2\pi}{k_{max}} = 3\pi \frac{\rho_\infty + \rho_j}{\rho_\infty \rho_j} \cdot \frac{\sigma_j}{u_j^2} \tag{4-27}$$

The mass rate of breakup of the jet, $\dot{m}_{br}$, per unit area of jet surface ($\lambda_{max} w$) is

$$\dot{m}_{br} \sim \pi \left(\frac{\lambda_{max}}{4}\right)^2 w_{o_j} \cdot m_{max}/(\lambda_{max} w) = \frac{\pi}{16} \rho_j \lambda_{max} m_{max} \tag{4-28}$$

or, from Equations (4-25) and (4-27),

$$\dot{m}_{br} \sim \frac{\pi^2}{8\sqrt{3}} \left(\frac{\rho_\infty}{\rho_j}\right)^{1/2} \rho_j u_j \tag{4-29}$$

where we invoked the approximation $\rho_j >> \rho_\infty$. It is remarkable to note that although surface tension places a limit on the rate of growth of the wave amplitude, it does not appear in the final expression for the rate of disintegration of the jet. An increase in σ_j, for instance, results in the ridges or drops being large but at the same time less of them are produced, with the result that the total breakup rate is unchanged.

There is no laboratory data on liquid jet disintegration rates with which Equation (4-29) can be validated. It is known from experiments with gas jets in air that the entrainment rate is given by an expression having the same functional form as Equation (4-29). Some measurements of entrainment with gas jets having a density different than the ambient gas have been made by Ricou and Spalding [24]. Assuming that the entrainment process with the miscible gas jet/air system is similar to the breakup of a liquid jet immiscible with the ambient fluid gives the following empirical equation:

$$\dot{m}_{br} = 0.08 \left(\frac{\rho_\infty}{\rho_j}\right)^{1/2} \rho_j u_j \qquad (4\text{-}30)$$

If such an interpretation proves to be correct, then a proportionality factor of the order of 0.1 is required in Equation (4-29) to bring the stability theory in line with the measurements.

Spencer et al. [25] performed experiments on molten corium jet-water interactions. In these tests a stream of molten corium was poured into a 32-cm deep pool of near-saturated water. The characteristic sizes of the quenched debris was determined by post test examination. The rate of steam generation was determined by measuring the rate of pressure rise in the test vessel. The latter measurement can be used to test Equation (4-30) by assuming that the molten corium torn from the jet was rapidly cooled to the saturation temperature. Then

$$\pi\, d_j\, L_j\, \dot{m}_{br} \left[h_{fs} + c_j(T_j - T_{sat})\right] = h_{fg}\, \dot{m}_s \qquad (4\text{-}31)$$

where d_j and L_j are the diameter and length of the jet, c_j and T_j are the heat capacity and temperature of the jet, and $\dot{m}_s$ is the steam generation rate. In writing the above energy balance it was assumed that the core of the jet is intact and not much reduced in diameter during transit through the pool. The test results showed this to be the case [25]. Inserting Equation (4-30) into Equation (4-31) and replacing the jet velocity u_j with the jet mass flow rate,

$$\dot{m}_j = \frac{\pi}{4} d_j^2\, \rho_j\, u_j \quad , \qquad (4\text{-}32)$$

gives

$$\frac{\dot{m}_s}{\dot{m}_j} = 0.32\, \frac{L_j}{d_j} \left[\frac{h_{fs} + c_j(T_j - T_{sat})}{h_{fg}}\right] \left(\frac{\rho_\infty}{\rho_j}\right)^{1/2} \qquad (4\text{-}33)$$

In applying Equation (4-33) one must decide whether to take ρ_∞ as the density of the water pool or to take ρ_∞ as the density of the steam produced by boiling. Epstein and Fauske [26] used linear Kelvin-Helmholtz instability analysis to examine the stability of a steam layer generated when a stream of molten reactor core material falls through water. From their work we can expect the density of the steam layer to govern the breakup of the jet if the thickness δ of the steam layer satisfies the inequality

$$\delta \gtrsim \frac{3\,(\rho_j + \rho_g)\,\sigma_j}{\rho_j\,\rho_g\,|u_j - u_g|^2} \tag{4-34}$$

where u_g is the opposing steam velocity.

Returning to the experiment of Reference [25], if the interfacial tension between corium and steam is taken comparable to the surface tension of molten UO_2, we estimate $\sigma_j = 0.45\ N\ m^{-1}$. The corium jet entered the water pool with the velocity $u_j = 3.7\ m\ s^{-1}$. Rapid steam generation was observed and based on the measured steam generation rate and the diameter of the test vessel a counterflow steam velocity $u_g = 35\ m\ s^{-1}$ was predicted by Spencer et al. With the steam density $\rho_g = 0.6\ kg\ m^{-3}$, corresponding to 1 atm pressure, we find that liquid is torn from the jet by the action of the surrounding steam if the steam film thickness $\delta > 1.5$ mm. Clearly this condition must have been satisfied in the corium quench experiment reported in [25] and the appropriate identification in Equation (4-33) is $\rho_\infty = \rho_g$. Inserting the corium mixture specific heat $c_j = 625\ J\ kg^{-1}$, the jet dimensions $L_j = 0.32$ m, $d_j = 0.022$ m, the jet temperature $T_j = 3080$ K, and the mean experimental density ratio $\rho_g/\rho_j = 1.1 \times 10^{-4}$ [25] into Equation (4-33), we predict

$$\frac{\dot{m}_s}{\dot{m}_j} = 0.044 \tag{4-35}$$

This prediction is a factor of two less than the value 0.089 inferred from the measured pressure-time history.

Considering the complexity of the jet quenching process, it is perhaps accidental that the steam production rate derived from experiment is so close to the rate predicted with Equation (4-33). Whether or not the reasoning which lead to the formula is correct must await future experimental work on the dispersion of hot molten jets in water. Nevertheless, this result appears to be sufficiently encouraging to warrant the use of Equation (4-33) in our study of the TMI core relocation event. Recall that the core relocation time based on plant instrumentation and present estimates was approximately 80 s. It is estimated that about 1.6×10^4 kg of molten core material drained downward from the core into the vessel lower head. Thus the melt mass rate of relocation was, on average,

$$\dot{m}_j = 200 \text{ kg s}^{-1} \tag{4-36}$$

The jet draining velocity u_j is dictated by a balance between the weight of the jet material and the retarding frictional stress at the surfaces of the fuel elements. The momentum balance for the jet flow through the fuel-element-bundle channels is

$$\frac{1}{2} f \rho_j u_j^2 = \frac{1}{4} \rho_j g D_h \tag{4-37}$$

where D_h is the hydraulic diameter of the bundle. Available channel flow data [27] suggest that the friction factor, f, may be obtained from the Blasius formula

$$f = 0.0791 \left(\frac{u_j D_h}{\nu_j} \right)^{-1/4} \tag{4-38}$$

Eliminating f between Equations (4-37) and (4-38) and solving the result for the jet velocity yields

$$u_j = 2.87 \frac{\nu_j}{D_h} \left(\frac{g D_h^3}{\nu_j^2} \right)^{4/7} . \tag{4-39}$$

With D_h = 1.32 cm for the TMI-2 core and $\nu_j = 6 \times 10^{-7}$ m^2 s^{-1}, we estimate a core material relocation velocity

$$u_j = 3.7 \text{ m s}^{-1} \tag{4-40}$$

We assume that the original molten stream that pours from the ceramic core cup is not redistributed into smaller individual streams. Then the effective diameter of the molten stream that flows downward through the intact channels is

$$d_j = \left(\frac{4}{\pi} \frac{\dot{m}_j}{u_j \rho_j} \right)^{1/2} = 0.083 \text{ m} \tag{4-41}$$

This result indicates that the mode of core material relocation through water may have been one of a relatively small diameter pour stream occupying no more than 20 percent of the flow area within a single fuel rod assembly.

Returning to Equation (4-33), we are now in a position to estimate the steam generation rate, assuming for the moment that the water below the molten core region was at the saturation temperature T_{sat} = 584 K. The range of a jet of d_j = 0.083 m falling through saturated water at 10 MPa will be shown later on to be about 6 m. Thus the core of the jet is essentially intact during transit through the approximately 1.8-m long, lower channel geometry. Accordingly we take L_j = 1.8 m, and calculate from Equation (4-33), together with Equations (4-36) and (4-41), that

$$\dot{m}_s = 110 \text{ kg s}^{-1} \tag{4-42}$$

during the core relocation. Comparison of the predicted steam generation rate with the value inferred from plant instrumentation of 9.5 kg s^{-1} [see discussion following Equation (4-20)] strongly suggests that the assumption of saturated water below the molten central region is not compatible with the recorded data. Highly subcooled water and little or no net steam generation during the period that the jet flowed to the bottom head seems

more probable. In this regard it is worth mentioning that Spencer et al. [25] also performed a test involving a corium pour into subcooled water. In contrast with the saturated condition, no net steam generation occurred.

4.3 Core Material Jet Breakup Length and Debris Characterization

It is evident from Equation (4-30) that the jet breakup velocity is

$$V_{br} = 0.08 \left(\frac{\rho_\infty}{\rho_j}\right)^{1/2} u_j \tag{4-43}$$

During the time interval

$$t = \frac{d_j}{2\, V_{br}} = \frac{6.25\, d_j}{u_j} \left(\frac{\rho_j}{\rho_\infty}\right)^{1/2} \tag{4-44}$$

the core of the jet will completely disintegrate. If the jet velocity remains constant during this period, the following approximation can be written for the intact length of the jet:

$$L = u_j t = 6.25\, d_j \left(\frac{\rho_j}{\rho_\infty}\right)^{1/2} \tag{4-45}$$

The jet breakup length is found to be independent of the jet velocity, provided that the velocity is high enough and the viscosity low enough to ensure that the surface waves are small compared with the diameter of the jet.

The available data on the range of water jets in air or water correlate well with Equation (4-45). The experiments of Oehler (1930; see Reference [28] for a summary of this work), for instance, showed that the core of a water jet in air extends about 150 jet diameters before it disintegrates. For this pair of materials $\rho_j/\rho_\infty \approx 10^3$ and Equation (4-45) gives $L/d_j = 197$. The disintegration of water jets in water ($\rho_j/\rho_\infty = 1$) has been studied

experimentally by Kuethe (1935; see Reference [28] for a summary of this work). He found that considerable disintegration has set in at 5 jet diameters. Formula (4-45) gives 7 jet diameters for the breakup length of water jets in water.

Let us now predict the breakup length of the molten core material stream in the TMI-2 vessel. Once again we first assume that the molten ceramic stream encounters saturated water during the fall stage. The critical steam layer thickness during the relocation is obtained by inserting the estimates $\sigma_j = 0.45\ N\ m^{-1}$, $u_j = 3.7\ m\ s^{-1}$ [see Equation (4-40)], $u_g = 0$, and $\rho_g = 55.36\ kg\ m^{-3}$ into Equation (4-34), from which we obtain

$$\delta = 1.8\ mm \tag{4-46}$$

It is clear that it makes sense to set $\rho_\infty = \rho_g = 55.36\ kg\ m^{-3}$ in Equation (4-45), since the thickness of the steam film in saturated boiling is much larger than 1.8 mm. The breakup length of the molten-core-material stream in saturated water is, then,

$$L = 6.25\ (0.083)\left(\frac{10^4}{55.36}\right)^{1/2} = 6.9\ m \tag{4-47}$$

Such a long melt stream would have resulted in a high impingement-type heat flux at the vessel lower head and a noncoolable melt layer, leading to likely failure of the head. The fact that this did not occur at the bottom of the TMI vessel lends additional support to the idea that highly subcooled water filled the lower region of the reactor vessel during the core relocation period.

If the water in the lower half of the vessel was sufficiently subcooled, then film boiling off the relocating fuel would not have been possible. Equating the thermal radiation heat flux across a postulated vapor film that covers the jet with the convective heat flux in the surrounding water, we find

$$e\sigma_B T_j^4 = \frac{f}{2} \rho_w c_w U_j (\Delta T)_{SUB} \tag{4-48}$$

where ρ_w and c_w are the density and heat capacity of the water and $(\Delta T)_{SUB}$ is the minimum subcooling required to maintain a vapor film on the downward moving jet. Note that the convection term on the right-hand side of Equation (4-48) neglects the effect of molecular processes. Reynolds' analogy between heat and momentum transfer is assumed to hold throughout the liquid boundary layer owing to the presence of the "lubricating" steam film. Solving Equation (4-48) for $(\Delta T)_{SUB}$ and using the parameter estimates T_j = 2800 K, e = 0.8, friction factor f = 0.005, ρ_w = 688 kg m^{-3}, c_w = 5728 J kg^{-1} K^{-1}, and u_j = 3.7 m s^{-1} provides a lower limit to $(\Delta T)_{SUB}$, namely

$$(\Delta T)_{SUB} = \frac{2 e \sigma_\beta T_j^4}{f \rho_w c_w u_j} = 76 \text{ K}, \tag{4-49}$$

If the subcooling in the lower region of the TMI vessel was of the order of 76 K or larger, the core material stream would not have been separated from the surrounding water by a steam film. Thus the waves on the jet would have amplified by the direct action of the water and should have disintegrated after falling a distance given by Equation (4-45) with $\rho_\infty = \rho_w$ = 688 kg m^{-3}, or

$$L = 2.0 \text{ m} \tag{4-50}$$

The significance of this result is that under subcooled conditions nearly complete jet breakup seems likely. The fact that the debris at the bottom of the TMI vessel is fragmented and coolable provides additional evidence that the core material relocated through subcooled water.

The size of the debris particles can be estimated by assuming that the average diameter of the particles torn from the jet, d, is of the order of the wavelength corresponding to the fastest growing wave on the jet surface. From Equation (4-27), we have

$$d = \lambda_{max} = \frac{3\pi(\rho_\infty + \rho_j)}{\rho_\infty \rho_j} \frac{\sigma_j}{u_j^2} \qquad (4\text{-}51)$$

This expression is practically the same as the Weber number criterion for the maximum stable drop size in a gas stream. Spencer et al. [25] reported that the limited breakup of corium in saturated water produced particle sizes consistent with Equation (4-51) when ρ_∞ is set equal to ρ_g. Of course, based on the previous discussion, the appropriate choice of ρ_∞ for TMI-2 conditions is ρ_w = 688 kg m^{-3}. Substituting the quantities σ_j = 0.45 N m^{-1} and u_j = 3.7 m s^{-1} into Equation (4-51), we get

$$d = 0.45 \text{ mm} \qquad (4\text{-}52)$$

Visual core bore inspections of the surface of the debris bed in the lower plenum revealed debris particles less than 1 cm in size but not nearly as small as the above prediction would lead us to believe. Considering the rough nature of the theory, the hope that it might coincide with the TMI-2 observations to any degree of accuracy would appear vain. On the other hand, final judgement regarding the accuracy of Equation (4-51) should be postponed until samples from the lower debris bed are obtained and a particle size distribution analysis is performed.

The maximum estimated height of the debris bed in the lower plenum is 0.762 m (see Reference [2]). An estimate of the heat flux at the top of the bed, $Q_H(1 - \epsilon)$, following core relocation is 5.7 x 10^5 W m^{-2}, assuming ϵ = 0.5. The dryout heat flux predicted with, say, Lipinski's model that includes both turbulent and laminar flow within the bed [7], and an average particle diameter given by Equation (4-52) is about 10^6 W m^{-2} [29]. Thus the particle size prediction 0.45 mm is not incompatible with the coolable debris bed at the bottom of the TMI-2 vessel.

Finally, it is worth noting that due to possible rapid surface solidification a thin skin of ceramic crust may cover the molten ceramic pour stream. Thus instead of capillary forces, we have a system where the jet surface tends to assume an equilibrium shape under the action of elastic

forces within the crust. Assuming that the effects of surface tension may be neglected, a rather straightforward analysis (in the spirit of Reference [30] for example) reveals that the expression for the wavegrowth constant is

$$m^2 = \frac{\rho_j \rho_\infty}{(\rho_j + \rho_\infty)^2} k^2 u_j^2 - \frac{Dk^5}{\rho_j + \rho_\infty} \tag{4-53}$$

where D is the flexural rigidity of the crust skin:

$$D = \frac{E\delta_c^3}{12 (1 - \varepsilon_p^2)} \tag{4-54}$$

Here E, ε_p and δ_c are the elastic modulus, Poisson's ratio and the instantaneous thickness of the crust.

Equation (4-53) replaces Equation (4-24). Interestingly enough, using Equation (4-53) to calculate λ_{max} and m_{max} we find that Equation (4-29) for the functional form of the breakup rate of the jet is still valid. Thus jet disintegration appears to occur at the same rate regardless of whether surface tension or elastic forces act to stabilize the motion. However, the time for an elastic wave to detach from the jet surface and the size of the particle torn from the jet are both greater than those associated with a capillary wave. Starting with Equation (4-53), the particle size produced by a jet with a crustal surface can be shown to be of the order of

$$d = \lambda_{max} = 2\pi \left(\frac{5 (\rho_\infty + \rho_j) D}{2 \rho_j \rho_\infty u_j^2} \right)^{1/3} \tag{4-55}$$

Accordingly, with $E = 0.8 \times 10^{11}$ Pa and $\varepsilon_p = 0.3$ for solid UO_2 [31], together with our previous estimates $\rho_\infty = \rho_w = 688$ kg m^{-3}, $\rho_j = 10^4$ kg m^{-3} and $u_j = 3.7$ m s^{-1}, we predict

$$d \approx 8 \text{ mm} \tag{4-56}$$

for the size of the particle torn from the pour stream by the buckling of a surface crust of thickness, say, δ_c = 10 μm. Comparing this value with the capillary theory result, Equation (4-52), it is apparent that the visual inspections of the lower plenum debris performed so far are more in line with an elastic theory of jet breakup than a capillary one.

It is obvious that a more complete theory of jet breakup with crust formation should include a prediction of the crust cover thickness, as opposed to treating δ_c as an adjustable parameter, as well as a derivation of the critical thickness of the steam layer which separates steam dominated wavegrowth from water dominated wavegrowth. While such a stability analysis is possible, further theoretical work of this nature is beyond the scope of the present report and, perhaps, would appear to be premature until more extensive and precise data samples are obtained from future explorations of the lower plenum region.

5.0 CONCLUDING REMARKS

Salient qualitative and quantitative features of the core relocation event during the TMI-2 accident have been shown to be compatible in most respects with a thermal/hydrodynamic sequence consisting of the following three stages: internal heating and melting of the consolidated region with little thermal communication between this region and the surrounding reactor coolant; collapse of the upper debris bed into the molten cavity formed within the consolidated region, together with boiling of the bed's interstitial water upon contact with the melt; and the displacement of the melt by the debris in the form of a narrow stream that erodes by Kelvin-Helmholtz instabilities on its way to the bottom of the vessel. Simple models have been utilized at each stage in an attempt to justify this conceptual picture of the core relocation event, but more information is needed, especially with regard to the breakup and mixing behavior of the relocating melt stream.

There has been extensive study of large coherent molten-core masses falling from the core region into the residual water pool in the lower plenum, particularly with regard to the possibility of steam explosions. However, a different and, perhaps, more likely mode of core material entry into water may have been revealed by the examinations of the TMI-2 reactor vessel, namely a relatively small diameter pour stream that was sustained for a minute or so. A key aspect of the relocation is, then, the lateral extent of the flow path through the fuel rod structure. Detailed mettallographic examinations of the fuel elements could prove invaluable, not only in terms of locating the actual relocation route but in resolving the issue of the timing and coherence of the relocation event.

It appears from the present work that the subcooling of the water in the lower half of the vessel was crucial to the formation of a coolable debris bed at the vessel bottom. Engineering analysis of the water temperature below the consolidated region should be carried out to establish the level of subcooling at the onset of the relocation event. An analysis of the recorded cold leg temperature transients may be helpful in this regard.

The breakup behavior of a molten core stream depends largely on the density of the ambient fluid. The influence of the steam layer is still somewhat unclear, and it may have a large effect on the melt stream breakup distance and the debris characteristics. Fundamental laboratory-scale experiments and accompanying theoretical work on the breakup and mixing behavior of hot jets flowing downward through water should be continued, with emphasis placed on determining the role of the steam phase produced by boiling off the surface of the jet.

Finally, there is important information yet to be gained by a thorough exploration of the lower plenum region. The particle size distribution may tell us whether or not subcooled water was instrumental in the formation of a coolable configuration. Recall that, according to theory, jet breakup is more efficient in a subcooled water environment than in the locally highly voided environment created in saturated water. An examination of the region close to the vessel wall and the vessel wall itself would also serve to indicate the extent of breakup of the pour stream. The character of the debris, that is a bed of solid particles in contact with the vessel wall versus a previously molten solid layer, will tell us whether the breakup of the jet was complete or a central core of melt channeled its way to the vessel bottom with little involvement in the breakup and quench process.

6.0 REFERENCES

1. J. Broughton, "Core Condition and Accident Scenario", Proceedings of the First International Meeting on the TMI-2 Accident, Conf-8510166, October 1985.

2. E. L. Tolman, J. P. Adams, J. L. Anderson, P. Kuan, R. K. McCardell, and J. M. Broughton, TMI-2 Accident Scenario Update, EGG-TMI-7489, December 1986.

3. C. M. Allison, S. T. Polkinghorne, and M. S. Sohal, SCDAP/MOD1 Analysis of the Progression of Core Damage During the TMI-2 Accident, EGG-SAR-7104, November 1985.

4. H. S. Carslaw and J. C. Jaeger, Conduction of Heat in Solids, 2nd edn., Oxford University Press, Oxford (1959).

5. P. Kuan, Core Relocation in the TMI-2 Accident, EGG-TMI-7402, November 1986.

6. P. Kuan, personal communication, June 1987.

7. R. J. Lipinski, "A Particle-Bed Dryout Model with Upward and Downward Boiling", ANS Trans. 35, 1980, pp. 358-360.

8. D. W. Akers, E. R. Carlson, B. A. Cook, S. A. Ploger, and J. O. Carlson, TMI-2 Core Debris Grab Samples - Examination and Analysis, GEND-INF-075, September 1986.

9. D. H. Cho, D. R. Armstrong, L. Bova, S. H. Chan, and G. R. Thomas, "Debris Bed Quenching Studies", in Proc. Int'l Mtg. on Thermal Nuclear Reactor Safety, NUREG/CP-0027, 2, February 1983, pp. 987-995.

10. T. Ginsberg, J. Klein, C. E. Schwarz, and J. Klags, "Transient Core Debris Bed Heat Removal Experiments and Analysis", in Proc. Int'l Mtg. on Thermal Nuclear Reactor Safety, NUREG/CP-0027, 2, February 1983, pp. 996-1010.

11. M. Jahn and H. H. Reineke, "Free Convection Heat Transfer with Internal Heat Sources, Calculations and Measurements", Proc. of the 5th Int'l Heat Transfer Conference, Tokyo, September 1974, Paper NC 2.8.

12. F. Mayinger, M. Jahn, H. H. Reineke, and V. Steinbrenner, Examination of Thermalhydaulic Processes and Heat Transfer in a Core Melt, BMFT RS 48/1, 1976, Institute for Verfahrenstechnik der T.U. Hanover.

13. J. R. Gabor, J. C. Cassulo, and P. G. Ellison, "Heat Transfer from Internally Heated Hemispherical Pools", paper presented at ASME/AIChE Nat'l Heat Transfer Conf., Orlando, Florida, July, 1980, Paper 80-HT-16.

14. F. A. Kulacki, review of Ref. [12] for the U. S. Nuclear Regulatory Commission under Contract AT(49-24)-0149, March, 1976.

15. R. Brandt and G. Neuer, "Thermal Conductivity and Thermal Radiation Properties of UO_2", J. Non-Equilib Thermodynamics, 1, 1976, pp. 3-23.

16. E. L. Tolman, R. P. Smith, M. R. Martin, R. K. McCardell, and J. M. Broughton, TMI-2 Core Bore Acquisition Summary Report, EGG-TMI-7385, September 1986.

17. P. N. Rowe, "Drag Forces in a Hydraulic Model of a Fluidized Bed - Part II", Trans. Inst. of Chemical Engineers, 39, 1961, pp. 175-180.

18. R. B. Bird, W. E. Stewart and E. N. Lighfoot, Transport Phenomena, 2nd edn., John Wiley, New York (1962).

19. O. A. Hougen and W. R. Marshall, "Absorption from a Fluid Stream Flowing Through a Stationary Granular Bed", Chemical Engineering Progress, 43, 1947, pp. 197-208.

20. N. Zuber, "On the Stability of Boiling Heat Transfer", Trans. ASME 80, 1958, pp. 711-720.

21. M. N. Hutcherson, Coolant Volume and Distribution in the TMI-2 Primary System Following Core Reflood and Slump, Unpublished FAI Report, 1986.

22. J. L. Anderson, personal communication, June 1987.

23. H. Lamb, Hydrodynamics, Dover, New York, 1945.

24. F. B. Ricou and D. B. Spalding, "Measurements of Entrainment by Axisymmetrical Turbulent Jets", J. Fluid Mech., 11, 1961, pp. 21-32.

25. B. W. Spencer, L. McUmber, D. Gregorash, R. Aeschlimann, and J. Sienicki, "Corium Quench in Pool Mixing Experiments", ANS Proc., 1985 Nat'l Heat Transfer Conf., ANS #700101, Denver, CO, August 1985.

26. M. Epstein and H. K. Fauske, "Steam Film Instability and the Mixing of Core Melt Jets and Water", ANS Proc., 1985 Nat'l Heat Transfer Conf., ANS #700101, Denver, CO, August 1985.

27. W. M. Rohsenow and J. P. Hartnett, eds. Handbook of Heat Transfer, McGraw Hill, New York, 1970, p. 64.

28. G. K. Batchelor, ed. The Scientific Papers of Sir Geoffrey Ingram Taylor, Vol. 3, 1963, pp. 304-305.

29. P. Kuan, personal communication, August 1987.

30. M. Epstein, "Stability of a Submerged Frozen Crust, J. Heat Transfer, 99, 1977, pp. 527-532.

31. Uranium Dioxide: Properties and Nuclear Applications, J. Belle, ed. U.S. Printing Office, 1961.